New BIOTECHNOLOGY 77 (2023) 20–29

Contents lists available at ScienceDirect

New BIOTECHNOLOGY

journal homepage: www.elsevier.com/locate/nbt

Crossing bacterial boundaries: The carbon catabolite repression system Crc-Hfq of *Pseudomonas putida* KT2440 as a tool to control translation in *E. coli*

Chunzhe Lu [a,*,1], Tiago P. Ramalho [a,1], Markus M.M. Bisschops [a], Rene H. Wijffels [a,b], Vitor A. P. Martins dos Santos [a,c], Ruud A. Weusthuis [a]

[a] *Bioprocess Engineering, Wageningen University and Research, 6700AA Wageningen, The Netherlands*
[b] *Faculty of Biosciences and Aquaculture, Nord University, N-8049 Bodø, Norway*
[c] *Lifeglimmer GmbH, Berlin, Germany*

ARTICLE INFO

Keywords:
Genetic toolbox development
Attachment site
Multiplex gene repression
Small RNA
Alkane monooxygenase
Medium chain fatty ester

ABSTRACT

As a global regulatory mechanism, carbon catabolite repression allows bacteria and eukaryal microbes to preferentially utilize certain substrates from a mixture of carbon sources. The mechanism varies among different species. In *Pseudomonas* spp., it is mainly mediated by the Crc-Hfq complex which binds to the 5′ region of the target mRNAs, thereby inhibiting their translation. This molecular mechanism enables *P. putida* to rapidly adjust and fine-tune gene expression in changing environments. Hfq is an RNA-binding protein that is ubiquitous and highly conserved in bacterial species. Considering the characteristics of Hfq, and the widespread use and rapid response of Crc-Hfq in *P. putida*, this complex has the potential to become a general toolbox for post-transcriptional multiplex regulation. In this study, we demonstrate for the first time that transplanting the pseudomonal catabolite repression protein, Crc, into *E. coli* causes multiplex gene repression. Under the control of Crc, the production of a diester and its precursors was significantly reduced. The effects of Crc introduction on cell growth in both minimal and rich media were evaluated. Two potential factors - off-target effects and Hfq-sequestration - could explain negative effects on cell growth. Simultaneous reduction of off-targeting and increased sequestration of Hfq by the introduction of the small RNA CrcZ, indicated that Hfq sequestration plays a more prominent role in the negative side-effects. This suggests that the negative growth effect can be mitigated by well-controlled expression of Hfq. This study reveals the feasibility of controlling gene expression using heterologous regulation systems.

Introduction

Carbon catabolite repression (CCR), as one of the predominant global regulatory mechanisms, ensures the hierarchical uptake of several carbon sources in bacteria and eukaryal microbes [1–3]. It allows microbes to maximize their growth rate by sequentially utilizing preferred carbon sources, resulting in a competitive advantage in environments with fluctuating and mixed nutrients [4–8]. CCR has been well investigated in Gram-negative bacteria, such as *Escherichia coli* and *Pseudomonas putida*, and Gram-positive bacteria, such as *Bacillus subtilis*. However prevalent, CCR did not evolve equally, and differences are observed between bacterial groups, both in terms of mechanisms and preferred carbon sources [5]. The global CCR regulation in *E. coli* primarily occurs at the pre-transcriptional level. The primary mediator is the phosphoenolpyruvate transferase system (PTS), which simultaneously transports carbohydrates and regulates the transcription of other sugar catabolic genes [5]. In addition to global CCR regulation, *E. coli* also demonstrates operon-specific mechanisms. These are mostly

Abbreviations: CCR, carbon catabolite repression; PTS, phosphoenolpyruvate transferase system; AS, attachment site; sRNAs, small RNAs; Atf1, alcohol acyltransferase; LB, Lysogeny broth; 3-MB, 3-methyl benzoate; NI, not induced; FID, flame ionization detector; TALE, transcription activator-like effector; CRISPRi, CRISPR interference.

* Corresponding author.
E-mail address: chunzhe.lu@rug.nl (C. Lu).
[1] These authors contributed equally.

https://doi.org/10.1016/j.nbt.2023.06.004

Available online 20 June 2023

responsible for the hierarchical uptake of non-PTS sugars, such as lactose, arabinose, and xylose. Glucose is observed as the preferred carbon source for *E. coli* [9]. The carbon uptake hierarchy in *Pseudomonas putida* differs from the conventional glucose prioritization observed in most bacteria [5,10]. Instead, the carbon assimilation order is as follows: organic acids and specific L-amino acids (proline, aspartate, asparagine, glutamate, glutamine and histidine); sugars such as glucose and fructose; other amino acids (arginine, lysine); benzoate and hydrocarbons [10]. This inverted CCR is likely an adaptation to soil colonization. In this habitat, *Pseudomonas putida* consumes compounds from organic decomposition and root exudates, which frequently have a higher concentration of organic acids than sugars [10,11].

Pseudomonal CCR is mainly governed by Crc [12], a protein modulating the expression of over 130 genes [13]. Crc works together with another protein, Hfq, forming a ribonucleoprotein complex at a target site located at the 5′ end of certain mRNAs [14] and blocking the formation of the translation initiation complex [15]. The target sequence, known as a Crc-Hfq attachment site (AS), varies in size and composition but is generally defined as AANAANAA [16–19]. These two factors (size and composition of AS), as well as the relative position of the AS to the target gene, contribute to the efficiency of translation repression. This allows *Pseudomonas* to differently modulate the

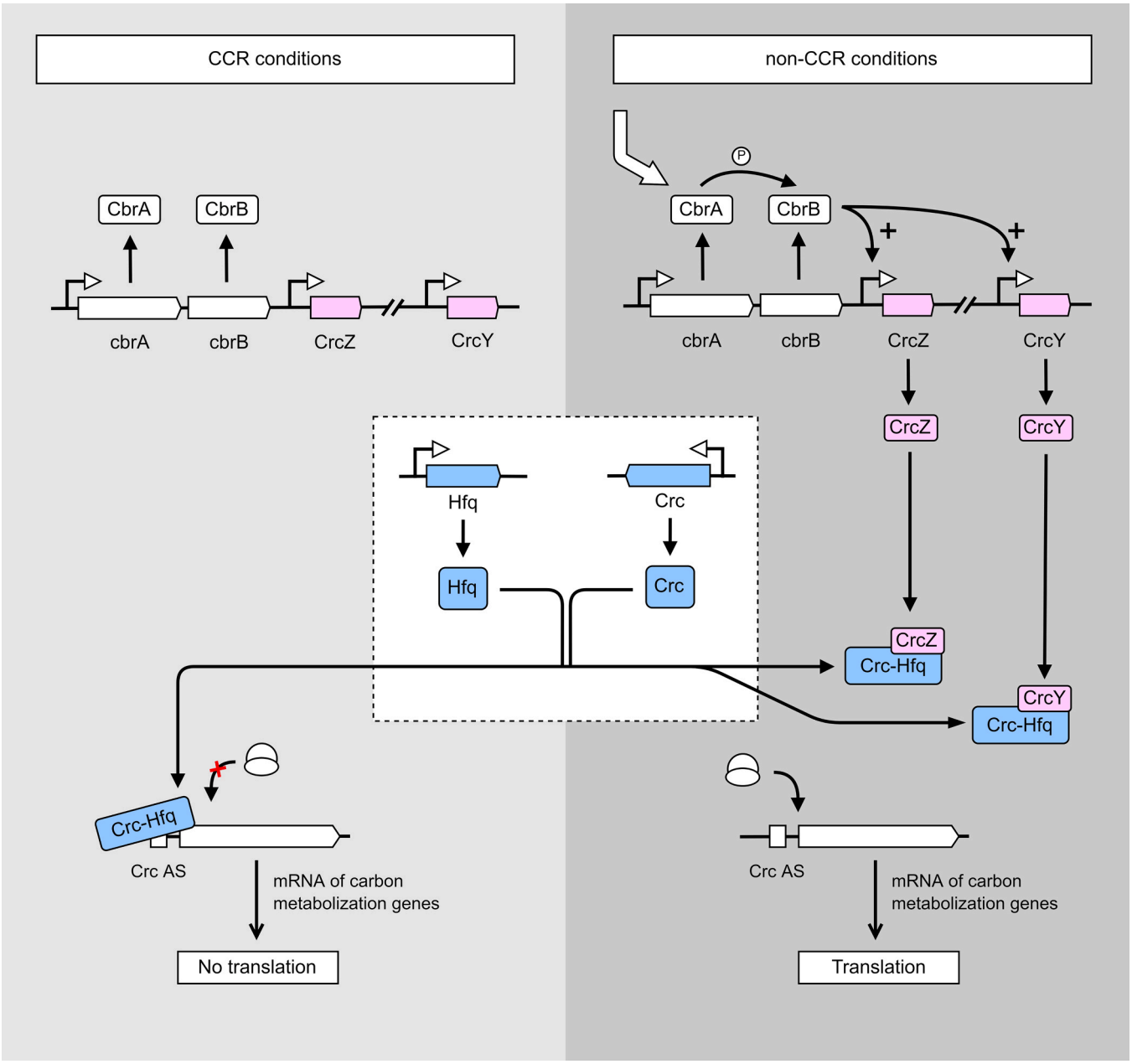

Fig. 1. Carbon catabolite repression by the Crc-Hfq regulatory network in *Pseudomonas putida*. The Crc and Hfq proteins are constitutively expressed. Under CCR conditions i.e., carbon abundance, the Crc-Hfq complex inhibits translation of genes involved in metabolism of less preferred carbon sources, by binding to Crc-Hfq attachment sites (AANAANAA) present in the 5 UTR of their mRNAs. Under non-CCR conditions, the two-component system CbrA/B detects an internal signal for carbon limitation (high 2-oxoglutarate/glutamine ratio) and activates the transcription of the CrcZ and CrcY sRNAs. These sRNAs contain multiple Crc-Hfq attachment sites, which sequester the Crc-Hfq complex allowing for the translation of carbon metabolization genes to occur. 2-OG: 2-oxoglutarate; CbrA: a sensor histidine kinase; cbrA: the gene coding CbrA; CbrB: an activator of σ^{54}-dependent promoters; cbrB: the gene coding CbrB; Crc: a mRNA binding protein serving as a global carbon catabolite repressor; CrcZ and CrcY: non-coding small RNAs regulating Crc; Hfq: an abundant bacterial RNA binding protein; Crc AS: Crc-Hfq attachment site.

expression level of numerous pathways by exploiting AS with varying repression efficiencies [16]. In *Pseudomonas* spp. such as *P. putida*, *P. fluorescens* and *P. syringae*, the control of Crc activity is mediated by the non-coding small RNAs (sRNAs) CrcZ and CrcY (Fig. 1) [16,20]. These sRNAs contain multiple Crc-Hfq attachment sites, which can sequester the Hfq protein and stop it from binding to target mRNAs [10, 20]. Overproduction of CrcZ or CrcY can significantly reduce catabolite repression. The expression of CrcZ and CrcY is activated by a two-component system CbrA/B [21]. This system responds to internal signals on carbon availability, such as the 2-oxoglutarate/glutamine ratio, promoting sRNA transcription when higher values, indicative of carbon limitation, are sensed [21].

Hfq proteins are present in diverse bacterial species, contributing to post-translational regulation networks [15,22,23]. Hfq from different bacterial species is expected to be still compatible with Crc to form a complex. For example, in an in vitro assay, Hfq from *E. coli* paired with Crc from *P. putida* to bind to the attachment site of mRNA sequences [15].

Considering these characteristics, and the broad applications of Crc-Hfq in *P. putida*, the Crc-Hfq complex holds the potential to be part of a general toolbox for post-transcriptional multiplex regulation. This molecular mechanism enables bacteria to rapidly adjust and fine-tune gene expression to the changing environment [24]. Because Crc-Hfq acts at the translational level, it can in theory deliver a faster response than other known gene regulation tools that act at the transcriptional level. Up-to-date research, however, focused on understanding CCR in its native host [12,25–27]. Previous studies have not investigated the impact of transplanting Crc between hosts such as from *P. putida* to *E. coli* on gene expression and cellular metabolism.

The introduction of Crc into a non-native host harboring Hfq might affect cells in two ways: off-target effects and/or Hfq shortage. The attachment site sequence targeted by Crc-Hfq is relatively short (~11nt) and therefore likely present in mRNAs of a non-native host. As a result, the introduced Crc might not only target mRNAs of interest (i.e., of the target gene(s)) but also bind to other mRNAs and thereby repress their translation, resulting in off-target effects. Introducing Crc may also sequester Hfq and thereby interfere with its normal regulation role. In *E. coli*, a limited availability of Hfq has been reported to reduce cell growth rate and final cell density [28].

Crc-Hfq attachment sites are present in the mRNAs of numerous genes, empowering these proteins to be global regulators in *Pseudomonas* spp. The alkane catabolic operon from *P. putida* GPo1 (also referred to as *Pseudomonas oleovorans*) is one of most well-investigated operons regulated by Crc-Hfq (Fig. 2). This pathway is divided into two gene operons: *alkBFGL* and *alkST* [29]. The AlkS protein is the activator of both operons. In the absence of n-alkanes, the *alkST* cluster is transcribed from the *PalkS1* promoter, which is negatively modulated by AlkS. AlkS is an unstable protein, and therefore maintained in limiting amounts [30], preventing the induction of the pathway in the absence of n-alkanes. When n-alkanes are present, AlkS activates the expression of both operons, *alkBFGL* and *alkST*, via the promoters *PalkB* and *PalkS2*, respectively. However, if a preferred carbon source such as glucose is present, translation of the AlkS protein is impeded. This repression of AlkS translation is imposed by the Crc-Hfq complex via binding to its attachment site (AATAATAATAA) in the AlkS mRNA [13]. Also, two other mRNAs, encoding the proteins AlkB, and AlkG from the pathway, contain Crc-Hfq attachment sites, further tightening the regulation [16]. As a result, n-alkanes are not significantly catabolised until the preferred carbon-source is depleted from the growth medium [10].

The monooxygenase system AlkBGT from this pathway has been combined with an alcohol acyltransferase (Atf1) to produce diesters in *E. coli* and *P. putida* [19,31,32]. In such a system, glucose is fed to provide acetyl-CoA and n-alkanes serve as precursors for the formation of diesters (1,6-diacetoxyhexane). However, the titerss of 1,6-diacetoxyhexane and its precursors are much lower in *P. putida* than in *E. coli*

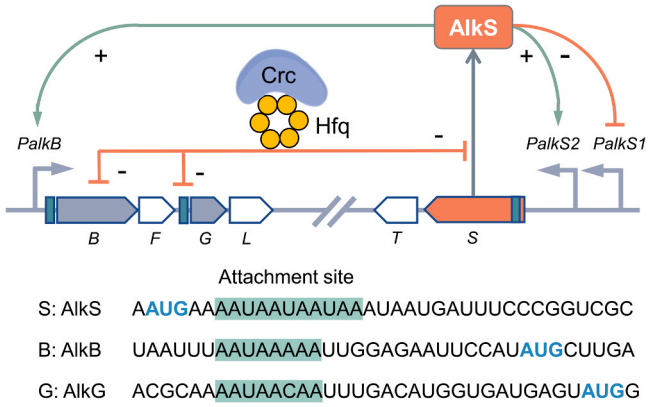

Fig. 2. Schematic illustration of catabolite repression of the alkane degradation pathway by the Crc-Hfq complex. AlkS: the activator of alkane degradation pathway; PalkS1: promoter of AlkS in absence of alkanes; PalkS2: promoter of AlkS with efficient transcription in presence of alkanes; Crc: the global regulator of carbon catabolite repression; Hfq: a bacterial RNA binding protein; B: AlkB, alkane monooxygenase; PalkB: promoter of AlkB; F: AlkF, rubredoxin 1 essential for AlkB activity; G: AlkG, rubredoxin 2; L: AlkL, outer membrane protein; T: AlkT, rubredoxin reductase; S: AlkS; + : activation; -: repression.

[19,31]. The Crc-Hfq regulation complex was assumed to be one of the main repressors causing glucose and n-alkanes to be assimilated sequentially rather than simultaneously in *P. putida*. Apart from alkane degradation, benzoate assimilation is another example where Crc-Hfq plays an important role. Crc-Hfq regulates benzoate degradation mainly by binding to the mRNA of BenR - the activator of the benzoate degradation genes [16].

In this study, the pseudomonal Crc-regulatory system is transplanted into a non-native host to assess its potential as a tool to regulate protein levels and production of diesters, but also its potential side effects. An *in-silico* analysis is conducted to determine the number and frequency of Crc-Hfq AS present in a group of organisms which natively harbor Crc or not. *E. coli* was chosen as an example to study the effects of the introduction of Crc on native metabolism in both minimal and rich media. To counter the growth-rate drop resulting from Crc introduction, the small RNA CrcZ was introduced to imitate its native Pseudomonal Crc-Hfq regulatory function in *E. coli*. Subsequently, using diester production as an indicator, the repression of Crc on the expression of multiple genes (AlkS, AlkB, AlkG) in *E. coli* were assessed. Green fluorescence protein (GFP) was fused with each target protein to monitor their expression. The feasibility of using Crc-Hfq in a non-native host for post-transcriptional multiplex regulation is demonstrated.

Materials and methods

Plasmid and strain construction

The *E. coli* and *P. putida* strains and plasmids used in this study are listed in Table 1. All primers used are listed in Table A.1. For plasmid construction, fragments were amplified using Q5® High-Fidelity DNA Polymerase (New England Biolabs, (NEB), Ipswich, MA, USA). HiFi assembly was conducted according to NEB's NEBuilder® HiFi DNA Assembly Reaction Protocol. The assembled products were transformed into *E. coli* 5α and the presence of correct constructs was verified with colony PCR [33]. Plasmids were isolated with the GeneJET Plasmid Miniprep Kit (Thermo Fisher Scientific, Waltham, MA, USA) and validated by sequencing (EZ-Seq, Macrogen, Amsterdam, The Netherlands). Correctly assembled plasmids were transformed into the intended strains. *E. coli* strains were made competent and transformed by chemical treatment [34]. *P. putida* KT2440 was transformed via electroporation. For this, an overnight 10 mL culture was pelleted (4255 x g for 5 min), resuspended in 1 mL of 300 mM sucrose solution and transferred

Table 1
Plasmids and strains used in this work.

Plasmids and Strains	Characteristics	Source
Plasmids		
pCOM	pMB1/rep ori, AlkS/PalkB inducible expression system, Kan^R	[35]
pCOM-AlkBGTL	pCOM harboring alkane degradation enzymes from *P. putida* GPo1 (AlkBGTL)	[31]
pCOM-AlkBGTL-Atf1	pCOM harboring alkane degradation enzymes from *P. putida* GPo1 (AlkBGTL) and alcohol O-acetyltransferase 1 (Atf1) from *Saccharomyces cerevisiae*	[19]
pCOM-AlkS:GFP	pCOM-AlkBGTL-Atf1 in which AlkS was fused with GFP	This study
pCOM-AlkB:GFP	pCOM-AlkBGTL-Atf1 in which AlkB was fused with GFP	This study
pCOM-AlkG:GFP	pCOM-AlkBGTL-Atf1 in which AlkG was fused with GFP	This study
pET26b	pBR322 ori, T7 inducible expression system, Kan^R	[36]
pET26b-CrcZ	pET26b harboring the small RNA CrcZ	This study
pSEVAb658	RSF1010 ori, XylS/Pm inducible expression system, Gm^R	[4]
pSEVAb658-Crc	pSEVAb658 harboring Crc	This study
pSEVAb658-GFP	pSEVAb658 harboring GFP	This study
pSEVAb658-Crc-GFP	pSEVAb658-Crc-GFP	This study
Strains		
Escherichia coli NEB®5-alpha	fhuA2 Δ(argF-lacZ)U169 phoA glnV44 Φ80Δ (lacZ)M15 gyrA96 recA1 relA1 endA1 thi-1 hsdR17	NEB
DH5α pSEVAb658-GFP	*E. coli* NEB®5-alpha carrying pSEVAb658-GFP	This study
Escherichia coli NEBT7 Express	fhuA2 lacZ::T7 gene1 [lon] ompT gal sulA11 R(mcr-73::miniTn10–TetS)2 [dcm] R(zgb-210::Tn10–TetS) endA1 Δ(mcrC-mrr)114::IS10	NEB
NEBT7-AlkBGTL-Atf1	*E. coli* NEBT7 Express carrying pCOM-AlkBGTL-Atf1	[31]
NEBT7-AlkBGTL-Atf1 +Crc	*E. coli* NEBT7 Express carrying pCOM-AlkBGTL-Atf1 and pSEVAb658-Crc	This study
NEBT7-GFP	*E. coli* NEBT7 Express carrying pSEVAb658-GFP	This study
NEBT7-GFP+Crc	*E. coli* NEBT7 Express carrying pSEVAb658-Crc-GFP	This study
NEBT7-AlkS:GFP	*E. coli* NEBT7 Express carrying pCOM-AlkS:GFP	This study
NEBT7-AlkS:GFP+Crc	*E. coli* NEBT7 Express carrying pCOM-AlkS:GFP and pSEVAb658-Crc	This study
NEBT7-AlkB:GFP	*E. coli* NEBT7 Express carrying pCOM-AlkB:GFP	This study
NEBT7-AlkB:GFP+Crc	*E. coli* NEBT7 Express carrying pCOM-AlkB:GFP and pSEVAb658-Crc	This study
NEBT7-AlkG:GFP	*E. coli* NEBT7 Express carrying pCOM-AlkG:GFP	This study
NEBT7-AlkG:GFP+Crc	*E. coli* NEBT7 Express carrying pCOM-AlkG:GFP and pSEVAb658-Crc	This study
Escherichia coli Top10	F- mcrA Δ(mrr-hsdRMS-mcrBC) Φ80lacZΔM15 Δ lacX74 recA1 araD139 Δ(araleu)7697 galU galK rpsL (StrR) endA1 nupG	Thermo Fisher Scientific
Top10-AlkBGTL-Atf1	*E. coli* Top10 carrying pCOM-AlkBGTL-Atf1	[37]
Top10-AlkBGTL-Atf1 +Crc	*E. coli* Top10 carrying pCOM-AlkBGTL-Atf1 and pSEVAb658-Crc	This study
Escherichia coli BW25113 (with integrated DE3 lysogen)	Wild-type *Escherichia coli* BW25113 with integrated DE3 lysogen	[38]
BW25113-GFP	*Escherichia coli* BW25113 (with integrated DE3 lysogen) carrying pSEVAb658-GFP	This study
BW25113-Crc	*Escherichia coli* BW25113 (with integrated DE3 lysogen) carrying pSEVAb658-Crc	This study
BW25113-CrcZ	*Escherichia coli* BW25113 (with integrated DE3 lysogen) carrying pET26b-CrcZ	This study
BW25113-Crc+CrcZ	*Escherichia coli* BW25113 (with integrated DE3 lysogen) carrying pSEVAb658-Crc and pET26b-CrcZ	This study

into a sterile 2 mL Eppendorf tube. Cells were washed twice (14000 rpm for 1 min), resuspended in 700 μL of 300 mM sucrose and placed on ice until the transformation step. To 100 μL aliquots of cells, 100 ng of plasmid were added and mixtures were transferred to prechilled 2 mm electroporation cuvettes. Electroporation was performed in a Bio-Rad Gene Pulser Xcell (Bio-Rad Laboratories, Temse, Belgium) at 2.5 kV, 200 Ω, 25 μF for 5 ms. Immediately after electroporation, 900 μL LB was added into cuvettes and mixed. Cultures were transferred into sterile 2 mL Eppendorf tubes and incubated for 1 h for recovery (30°C, 250 rpm). Afterwards, 20 μL of culture were spread on LB agar plates with the appropriate antibiotic (50 μg/mL kanamycin or 10 μg/mL gentamicin). Colony PCR and sequencing were conducted to verify the presence of the plasmids.

Growth media and cultivation conditions

The culture media used in this study were Lysogeny broth (LB), M9 Glucose, and M9 Xylose. The standard LB medium (Difco, Sparks, MA, USA) was employed. The M9 minimal medium base composition was as follows: 1x M9 minimal salts, 0.241 g/L $MgSO_4$, 1 x trace elements and vitamins [32,39,40]. A carbon source was then added to make the complete M9 media: M9 Glucose (4.5 g/L glucose) and M9 Xylose (12 g/L xylose).

E. coli strains were cultivated at 37°C, 250 rpm, except for the experiment where the effect of Crc introduction on diol bioproduction was evaluated, which was cultivated at 30°C, 250 rpm. Pre-cultures were inoculated in LB medium from frozen glycerol stocks and incubated overnight. Cells were then transferred into the culture medium at an OD_{600} of 0.1, again except for the diol production experiment (starting OD_{600} of 0.167). Cells were transferred directly to M9 Glucose and LB medium. For growth rate experiments in M9 Xylose, cells were first washed twice with M9 Xylose medium. Gentamycin and kanamycin were added at 10 μg/mL and 50 μg/mL if needed. Unless stated otherwise, strains with the XylS/Pm system (Table 1) were fully induced after 2 h incubation by the addition of 1 mM 3-methylbenzoate (3-MB). Likewise, the AlkS/PalkB system was induced after 2 h incubation by the addition of 0.025% v/v dicyclopropylketone. Strains containing the T7 system were fully induced immediately with 0.1 mM isopropyl β-D-1-thiogalactopyranoside (IPTG). All experiments were carried out in biological triplicates.

Growth assay of E. coli expressing Crc on both minimal and rich media

The BW25113-Crc strain was cultivated in 50 mL of minimal medium (M9 Xylose) in a 250-mL shake flask to assess potential effects of Crc on *E. coli* metabolism. Strains BW25113, BW25113-GFP and BW25113-Crc (NI, not induced) were used as controls. Induction was triggered by adding 1000 μM 3-MB at the 2 h time point. Cultures were sampled every other hour for cell density measurement until the stationary phase was reached.

Adding to the characterization of the potential effects of Crc on *E. coli* metabolism, the BW25113-Crc strain was cultivated in 50 mL of LB medium in a 250-mL shake flask. Different amounts of Crc were tested via partial induction of the XylS/Pm system with concentrations of 1000, 100 and 50 μM of 3-MB. Wild-type (BW25113), GFP-expressing (BW25113-GFP) and non-induced (BW25113-Crc NI) controls were

included for comparison. Cultures were induced immediately after inoculation. Samples were taken every hour until the stationary phase was reached. Optical density (OD_{600}) was immediately measured.

Cell density was monitored by measuring the absorbance at 600 nm (OD_{600}) using a HACH DR6000 Spectrophotometer (Hach, Manchester, UK). Different growth phases were identified by applying a natural logarithm to the OD_{600} data i.e. semi-ln plot. Growth rates were calculated from the exponential growth phase - linear section in natural logarithm plot with a positive slope and an $R^2 \geq 0.95$. The lag phase corresponded to the section preceding the exponential phase. The difference in growth rate between conditions was assessed using a one-way ANOVA followed by Tukey's multiple-comparison test (threshold was an adjusted p-value = 0.05).

Co-expressing Crc and CrcZ in E. coli

The plasmid pET26b-CrcZ was separately introduced in BW25113 and BW25113-Crc, resulting in BW25113-CrcZ and BW25113-Crc+CrcZ. Various Crc to CrcZ ratios were tested by expressing Crc in different amounts (500, and 1000 μM 3-MB) in combination with varying CrcZ by adding several IPTG concentrations (0, 10, 100 and 500 μM). Non-induced controls were included to account for the potential metabolic burden of two plasmids. Moreover, the following controls were added 1) BW25113, 2) BW25113-GFP (1000 μM 3-MB), 3) BW25113-Crc (0, 500, and 1000 μM 3-MB), 4) BW25113-CrcZ (500 μM IPTG), 5) BW25113-Crc+CrcZ with 3-MB (0 μM) and IPTG (0 μM). Tests were carried out in 48-well plates with a working volume of 500 μL LB. Growth dynamics for all conditions were determined by measuring OD_{600} every hour in the Tecan Infinite® 200 PRO microplate reader (Tecan Group Ltd., Männedorf, Switzerland), 25 flashes per read) until the exponential phase was reached. Growth rates in the exponential phase were calculated. A one-way ANOVA followed by Tukey's multiple-comparison test (adjusted p, 0.05) was applied to assess significance of growth differences.

Diol production in E. coli co-expressing AlkBGTL-Atf1 and Crc

A resting-cell assay was implemented to assess diol production. Product titers were measured for NEBT7 and Top10 strains expressing the diol production module, consisting of *Pseudomonas putida* Gpo1 AlkBGTL and *Saccharomyces cerevisiae* Atf1, with and without Crc. Cells were first cultivated in 30 mL of M9 Glucose to express the target proteins. After 4–6 h of incubation ($OD_{600} \geq 0.4$), the cultures were collected and centrifuged at 4255 x g for 10 min. The pellet was resuspended in resting-cell buffer (10 g/L glucose, 0.241 g/L $MgSO_4$ and 500 mL/L 0.1 M KPi pH 7.4) to a concentration corresponding to 1 g_{cdw}/L, based on a previously determined conversion factor (0.32 OD_{600} / g_{cdw}/L) [36]. 900 μL of cell suspension was then transferred into a Pyrex tube in triplicate and n-hexane was added to a final concentration of 76 mM. Cultures were incubated for 20 h, after which the reaction was stopped by placing the cells on ice for 10 min. Samples were extracted according to a previously reported method [19] and analyzed via gas chromatography. The significance of the difference between measured product titers was determined using a two-way ANOVA followed by Tukey's multiple-comparison test (threshold: adjusted p-value, 0.05).

Analytical assays

Fluorescence measurement

For each time-point, 2 mL samples were taken, washed once and resuspended in phosphate-buffered saline (PBS) to a final OD_{600} of 0.75 (8050 x g for 1 min). 200 μL per sample were distributed into a 96-well no-lid plate in triplicate. The fluorescence was measured in a BioTek™ FLx800™ microplate fluorescence reader (Gain 35). Relative fluorescence was calculated using the following formula: [41].

$$Relative \quad fluorescence(\%) = \frac{RFU_S/OD_S}{\mathrm{RFU_P}/\mathrm{OD_P}} \times 100$$

RFU and *OD* stand for relative fluorescence units and OD_{600} of the sample (*S*) and positive control (*P*). Crosstalk was determined not to be significant as no fluorescence was measured in negative controls adjacent to positive controls.

Gas chromatography analysis

A 1 μL sample was injected into an Agilent 7890 A gas chromatograph (Agilent Technologies, Santa Clara, CA, USA) with a flame ionization detector (FID) according to the previously reported method [31]. Instrument parameters were set at: injection temperature of 300 °C; pressure of 36.87 kPa; H_2 as a carrier gas; gas flow rate of 1.00 mL/min; average velocity of 18.92 cm/s. Product quantification was achieved with a set temperature program on a HP-5 column [19]. Simultaneously, calibration curves were prepared for 1-hexanol, hexyl acetate, 6-hydroxyhexyl acetate and 1,6-diacetoxyhexane.

Screening of genome database for Crc-Hfq attachment sites and blasting of Hfq protein sequences from different organisms

The numbers of general (AANAANAA), BenR (AACAATAA) and AlkS (AATAATAATAA) Crc-Hfq attachment sites were quantified in the genomes of *E. coli* BW25113, *P. putida* KT2440 and other organisms of interest. Those bacterial species were selected according to [42], a review paper on Crc-Hfq regulation in *Pseudomonas*. The *in-silico* screening was carried out using the SnapGene® software (GSL Biotech LLC, Boston, MA, USA). In addition, the relative position to coding genes was determined for the BenR attachment site. Genes where this site was present between 40 bp upstream and 15 bp downstream of the start codon were noted as likely targets for Crc-Hfq repression [43]. The screening was repeated considering the relative position of the BenR attachment site to the Shine-Dalgarno sequence (AGGAGG) instead of the start codon (ATG). The BenR attachment site was chosen for these tests as it has the highest binding efficiency by Crc-Hfq and therefore could lead to the strongest off-target effects [16]. Finally, the frequency of Crc-Hfq attachment site was calculated for every organism by dividing the total number of general Crc-Hfq attachment sites by the genome size.

Hfq protein sequences from different organisms (Table A.2) were blasted with the blastp program against Hfq protein sequence from *P. putida* KT2440 at the server of the National Center for Biotechnology Information (http://www.ncbi.nlm.nih.gov/blast).

Results and discussion

In-silico screening of the occurrence and location of attachment site sequences

To assess the effects of transplanting the Crc repression system into a non-native host, the likelihood of off-target effects was studied first. As such, the number and frequency of AS sequences were determined *in silico* for *P. putida* KT2440, *E. coli* BW25113 and other organisms of interest. Strains were divided into two groups based on the presence of Crc (Table 2). As a eukaryotic model organism, *Saccharomyces cerevisiae* BY4742 was included because it contains the Lsm protein (a Hfq homolog) [44] which might be able to form a complex with Crc for gene repression.

For species harboring Crc, the relative frequency of general attachment sites is comparable (~0.03%, Table 2). In contrast, organisms without Crc regulation contain a much higher AS frequency (0.06–0.5%, Table 2). It is likely that through evolution, in the group of species equipped with the Crc-Hfq regulation mechanism, counter-selection

Table 2
Presence and similarity of Hfq and of occurrence of general (AANAANAA), BenR (AACAATAA) and AlkS (AATAATAATAA) Crc-Hfq attachment sites (AS) in different organisms.

Organism	Hfq or its homolog[a]	Identity to Hfq from *P. putida* KT2440 (%)	Crc-Hfq general AS amount	Percentage of AS frequency per total bp (%)[b]	BenR AS amount	AlkS AS amount
Strains using Crc as a gene repression tool						
Pseudomonas putida KT2440	+	100	2043	0.033	62	3
Pseudomonas aeruginosa PAO1	+	85	1403	0.022	49	1
Pseudomonas oleovorans T9AD	+	87	1404	0.025	48	0
Pseudomonas fluorescens ATCC 13525	+	87	2756	0.042	107	0
Pseudomonas syringae pv. tomato str. DC3000	+	87	2752	0.036	123	3
Azotobacter vinelandii DJ	+	87	1456	0.027	53	1
Strains without Crc regulation						
Escherichia coli BW25113	+	87	5368	0.1159	288	9
Bacillus subtilis 168	+	45	11,912	0.2824	293	17
Corynebacterium glutamicum ATCC 13032	-	-	2132	0.064	75	1
Vibrio cholerae MS6	+	85	4957	0.1231	247	3
Saccharomyces cerevisiae BY4742	+	n.s.[c]	62,201	0.51	1921	583

[a] + : Hfq or a homolog is present; -: Hfq or a functional homolog is absent.
[b] The percentage of motif frequency per total bp (%) is the number of general motifs divided by the total base pairs multiplied by 100%.
[c] n.s.: no significant similarity.

against random attachment sites has resulted in maintaining only those with a function. This ensured that Crc-Hfq serves as an efficient and accurate gene repression tool, without off-target effects. In addition, Hfq proteins from Crc-carrying species share 85–87% identity, indicating conservation among these species (Table 2). Hfq from *P. putida* KT2440 shares 87%, 85% and 45% identity with Hfq from *E. coli* BW25113, *Vibrio cholerae* MS6, and *B. subtilis* 168 respectively, suggesting their potential to pair with Crc. For Hfq from *E. coli* in particular, it has been shown that Crc can pair with it to bind to attachment sites of mRNA sequences in an in-vitro test [15]. Lsm1 is a functional homolog of Hfq in *Saccharomyces cerevisiae* [45]. Therefore, it was also evaluated, although lacking significant similarity with Hfq from *P. putida* KT2440.

In comparison to *P. putida* KT2440, more than twice as many general Crc-Hfq AS sequences (AANAANAA) were present in the genome of *E. coli* BW25113 (Table 2). The difference increased when genome size was considered. *E. coli* BW25113 contained on average one Crc-Hfq AS sequence per 0.85 kb, whereas *P. putida* KT2440 only had one per 3 kb. The same relationship was found for the number of BenR (AACAATAA) and AlkS (AATAATAATAA) AS sequences. For *E. coli* BW25113, 24.7% of the 288 occurrences were in a position where Crc could cause gene repression, i.e. up to 40 bp upstream and 15 bp downstream of a start codon [16,43]. Contrastingly, this was the case for 66.1% of the 59 occurrences of BenR attachment site in *P. putida* KT2440 (excluding 2 matches within *CrcZ* and 1 match in *CrcY*). A list of these 36 genes is provided in. The difference was more significant taking into consideration the relative position of the BenR AS sequence to the Shine-Dalgarno sequence (AGGAGG) instead of the start codon. In this case, *P. putida* KT2440 presented a much higher percentage of probable Crc-repression targets (6.45%) than that of *E. coli* (1.04%). This again suggests that the location of attachment sites in *P. putida* is more purposive than that in *E. coli*. The occurrence of off-target effects is likely greater in organisms lacking Crc-based regulation given that their genome is not evolved to avoid non-specific repression. This may pose a barrier in transplanting Crc to this group of organisms depending on the location and binding-strength of the targeted attachment sites.

Effects of Crc on native E. coli metabolism

The *in silico* quantification of Crc-Hfq AS sequences demonstrates the possibility of off-target effects when Crc is expressed in other hosts harboring Hfq, but that do not rely on Crc regulation. However, this analysis does not necessarily have to be translated to in vivo effects, nor does it inform about the potential impacts of Hfq sequestration on native metabolism. Considering the similarity of Hfq from *P. putida* and *E. coli* [15], pseudomonal Crc was introduced in *E. coli* BW25113 to evaluate these factors. The growth dynamics of this strain on both a minimal medium (M9 Xylose) and a rich medium (LB) were investigated.

Crc reduces E. coli BW25113 specific growth rate

The specific growth rate of strain BW25113-Crc on M9 Xylose medium was two-fold lower when Crc was expressed (induction by 1000 μM 3-MB) compared to BW25113 and BW25113-GFP (adjusted p-value < 0.05) (Fig. 3a). The final cell density was not affected by Crc expression, all cultures reached a final OD_{600} above 4.

Expression of Crc significantly extended the lag phase (Fig. 3b). For the two negative controls (BW25113 and BW25113-GFP), the lag phase was surpassed under 10 h, which took over 20 h for the BW25113-Crc strain. This increase in lag phase duration cannot be explained by the decrease in growth rate. The introduction of Crc likely interferes with the expression of essential genes to overcome the lag phase associated with the transfer from LB to M9 Xylose medium.

Growth dynamics of E. coli BW25113 expressing Crc on a rich medium

On LB medium, specific growth rates were also reduced when Crc was expressed (Fig. 4a). The effects of different Crc expression levels on cell growth were evaluated. To determine the sensitivity of the XylS/Pm expression system, the relative fluorescence of a strain harboring the gene encoding GFP under control of the Pm promoter was determined in the presence of different concentrations of the inducer 3-MB. At 1000 μM 3-MB, the expression level of GFP was defined as 100%. GFP Expression levels of 38%, 23% and 2% were obtained when 100 μM, 50 μM and 0 μM 3-MB were added respectively (Suppl. Fig. A1). The wild-type BW25113 and BW25113-GFP, as negative control strains, reached stationary phase after 6 h on LB medium, while a fully induced (100%) Crc-expressing strain BW25113-Crc required double that time (Fig. 4b). Additionally, the final cell density was inversely related to the expression level of the Crc protein (Fig. 4b). Intermediate expression levels of Crc (38% and 23%) resulted in a more moderate decrease in both specific growth rate and final cell concentration. These are the only two conditions found not to differ significantly from each other (Tukey test, adjusted $p < 0.05$).

The introduction of Crc in *E. coli* BW25113 negatively affected cell growth in both minimal and rich medium. Two main growth interference hypotheses were proposed: 1) off-target effects and 2) Hfq

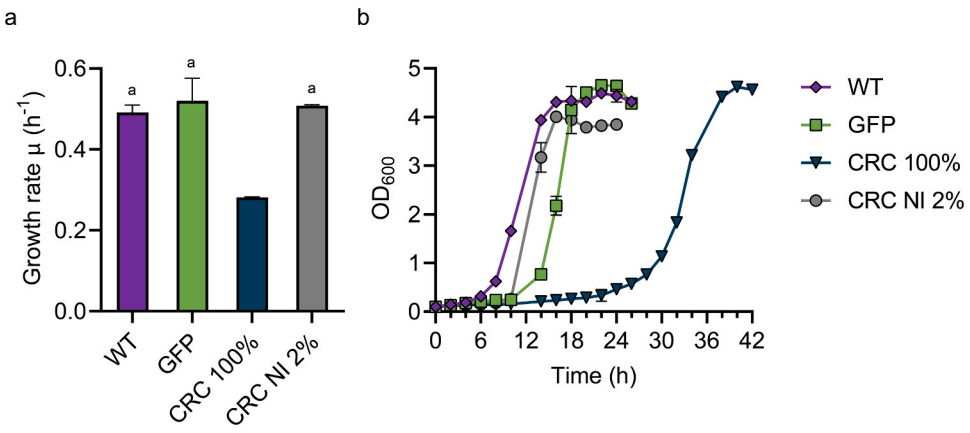

Fig. 3. The effect of Crc on *E. coli* specific growth rate (a) and dynamics (b) on a minimal medium (M9 Xylose 12 g/L). The tested strains are BW25113 (WT), BW25113-GFP (GFP), non- and fully-induced BW25113-Crc (Crc NI (non-induced) 2% and Crc 100%). Under non-induced conditions, there is a leaky expression, corresponding to 2% of expression level. Error bars display standard deviation over three biological triplicates. Growth rates of the strains WT, GFP and Crc NI were not significantly different from each other (indicated by 'a', Tukey test, adjusted p-value > 0.05). The growth rate of BW25113-Crc 100% was significantly reduced compared to all other conditions.

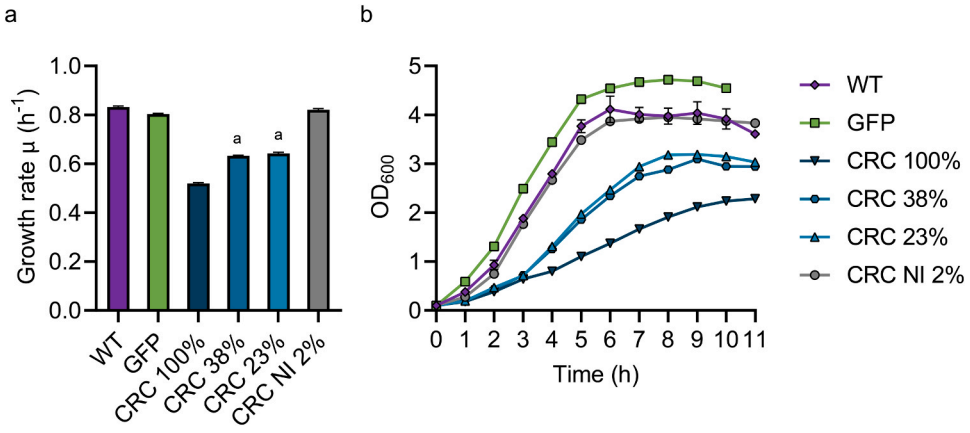

Fig. 4. The effect of Crc on *E. coli* growth rates (a) and dynamics (b) on a rich medium (LB). The tested strains are BW25113 (WT), BW25113-GFP (GFP) and BW25113-Crc (Crc). The latter was induced with different concentrations of 3-MB (0, 50, 100 and 1000 μM) resulting in varying Crc expression levels (2%, 23%, 38% and 100%). The relative protein production was quantified via an analogous GFP test (Fig. A1). Error bars display standard deviation over three biological triplicates. Conditions that do not share a letter are significantly different (Tukey test, adjusted p, 0.05). Only the conditions expressing 38% and 23% of Crc were found not to be significantly different. 3-MB: 3-methylbenzoate.

shortage. Crc could have inhibited *E. coli*'s growth via off-target effects. As such, the extent to which growth may be affected by Crc depends on the number and location of off-target Crc-attachment sites. Apart from the off-target effects, Crc could also be inhibiting growth by sequestering too much of the limited native Hfq pool, which is necessary for sRNA-based regulation in *E. coli* [46]. In that case, growth deregulation would not be caused directly by Crc, but rather by lack of Hfq. It has been demonstrated that the deletion of Hfq causes both a reduction of growth rates and final cell density [28].

Co-expression of Crc and CrcZ further reduces E. coli specific growth rates

To determine which of the two Crc putative effects on growth is more significant, the pseudomonal CrcZ gene was co-expressed with Crc in *E. coli* at different ratios. In *Pseudomonas*, the sRNA CrcZ controls Crc-Hfq availability by sequestering it, thereby relieving catabolite repression [20]. This implies that co-expression of Crc and CrcZ should mitigate off-target effects, but could aggravate Hfq sequestration effects. Therefore, if specific growth rates improve in the presence of CrcZ, it would suggest that off-target effects lead to the growth inhibition. However, if the opposite is observed and specific growth rates decrease even further when Crc and CrcZ are co-expressed, it would indicate that Hfq shortage causes the decrease in growth rates.

CrcZ was expressed from a pET26b plasmid in strain BW25113-Crc+CrcZ. Two expression levels (100% and 38%) of Crc were tested. The expression level of CrcZ was tuned by using different amounts (0, 10, 100 and 500 μM) of the inducer IPTG. With 100% expression of Crc, any expression of CrcZ resulted in a decrease of the specific growth rate (adjusted p-value < 0.05) (Fig. 5). The reduction furthermore correlated with the induction level of CrcZ, indicating that increasing amounts of

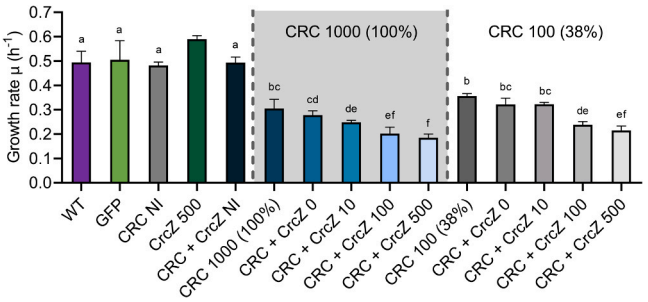

Fig. 5. The effects of co-expressing Crc and CrcZ on *E. coli* specific growth rates on LB medium. Tests were separated into three groups: a negative control group, experiments with 100% Crc expression or with 38% Crc expression. The negative control group consisted of BW25113 (WT), induced BW25113-GFP (GFP), non-induced BW25113-Crc (Crc NI), induced BW25113-CrcZ (500 μM IPTG), and non-induced BW25113-Crc+CrcZ (Crc+CrcZ NI). The Crc 100% group consisted of fully-induced BW25113-Crc (Crc 100%), BW25113-Crc+CrcZ (CRC 100%, CrcZ 0, 10, 100, 500 μM IPTG). The Crc 38% was made up of partially induced BW25113-Crc (Crc 38%), BW25113-Crc+CrcZ (CRC 38%, CrcZ 0, 10, 100, 500 μM IPTG). Error bars display standard deviation of biological triplicates. Conditions that do not share a letter are significantly different (Tukey test, adjusted p-value < 0.05).

CrcZ resulted in a progressively stronger growth inhibition. The same trend was found under the 38% Crc expression condition (Fig. 5). Individually, CrcZ did not inhibit growth as the BW25113-CrcZ strain had a similar growth rate as the reference strain BW25113. Furthermore, the growth rates of the BW25113-Crc and BW25113-Crc+CrcZ in absence of inducer (NI) were not significantly different (adjusted p-

value > 0.05). This showed that the metabolic burden of carrying two plasmids did not explain the specific growth rate reduction, but that it was caused by the combinatorial expression of Crc and CrcZ. These findings strongly indicate that Hfq sequestration is the main cause of growth inhibition caused by Crc.

Thus, most of the inhibitory effects of Crc can potentially be mitigated by overexpressing Hfq, allowing for its native pool to remain stable. It is clear that additional engineering efforts are needed to render this Crc-Hfq system a mature and well-controlled toolbox for general purposes.

Impact of Crc introduction on diol production in E. coli

To assess whether Crc could impose multiplex gene repression, the alkane monooxygenase module (AlkBGTL) from *P. putida* GPo1 combined with alcohol acyltransferase Atf1 from *S. cerevisiae* (Fig. 6a) was expressed in *E. coli* for diol production in the presence or absence of Crc. Here, the rationale was that *E. coli's* native Hfq could bind to the attachment sites together with Crc. Within the alkane monooxygenase module, the expression of key genes (AlkS, AlkB, AlkG, Atf1) is regulated by Crc-Hfq. The production of diols and its intermediates was monitored as an indicator of gene repression.

Co-expression of Crc with AlkBGTL-Atf1 in both *E. coli* NEBT7 and Top10 strains significantly reduced total product formation from n-hexane compared to strains only harboring AlkBGTL-Atf1 (adjusted p-value < 0.05) (Fig. 6b). NEBT7-AlkBGTL-Atf1 +Crc showed a 59% drop in total product concentration from 8.7 mM to 3.6 mM. Similarly, for Top10-AlkBGTL-Atf1 +Crc the concentration of total products decreased from 3.1 mM to 0.9 mM, corresponding to a decrease of 72%. This was expected as the genes AlkBGTL-Atf1, are under control of the AlkS/PalkB inducible promoter system. Within this system, the mRNA encoding AlkS, the activator of the whole operon, contains an attachment site. Therefore, Crc-mediated repression lowers available levels of the AlkBGTL-Atf1 enzymes because it limits the translation of AlkS and thereby transcription of the AlkB, AlkG and Atf1 genes. Additionally, translation of AlkB and AlkG mRNAs is reduced, because they contain their own attachment sites [16].

Crc introduction reduced overall product formation, but not all product concentrations were affected equally, which implies some conversions were more impacted by Crc (Fig. 6b). The accumulation of

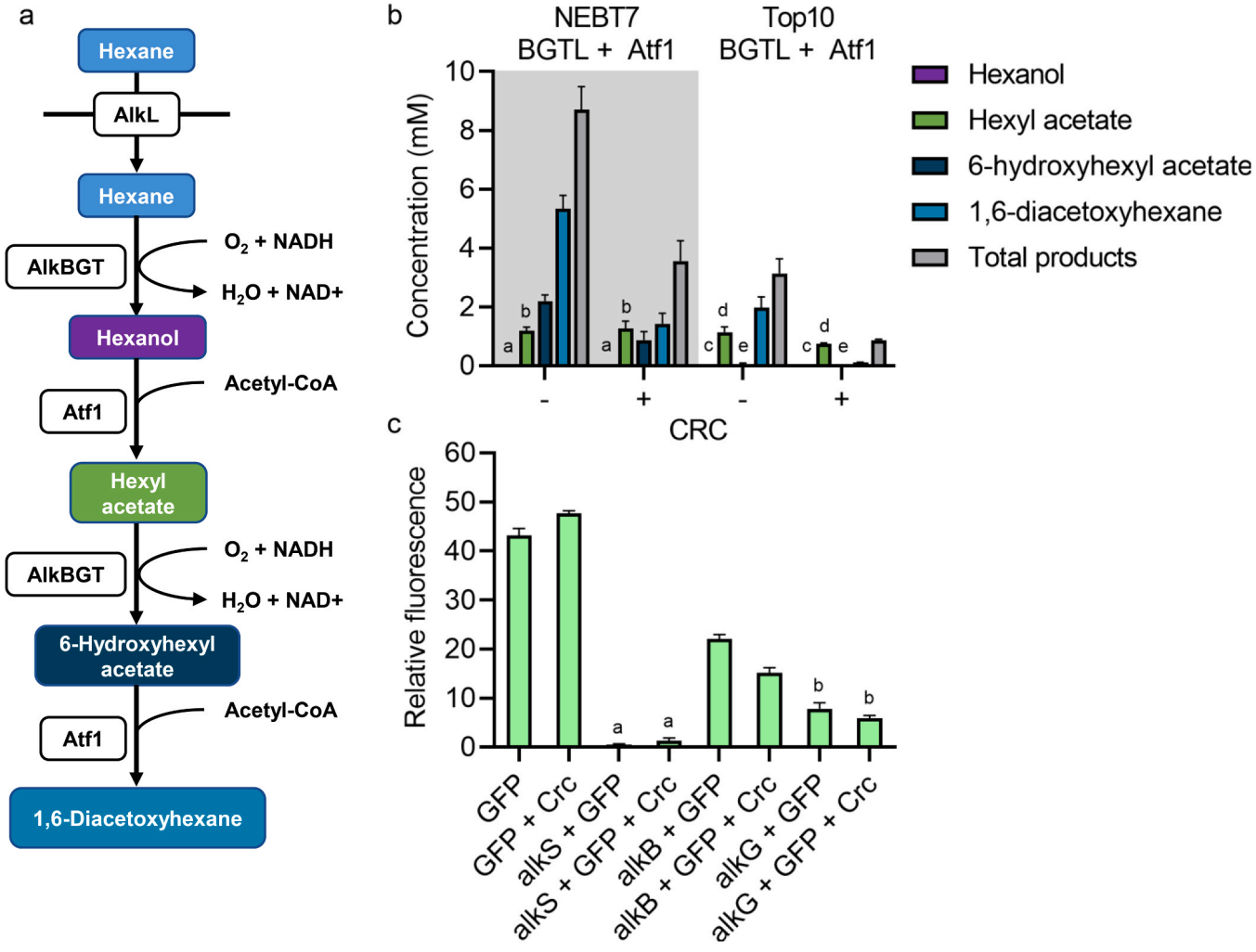

Fig. 6. The effect of Crc introduction on gene expression in *E. coli*. (a) Schematic of the diol synthesis pathway consisting of alkane oxidation module (AlkBGTL) and esterification module (Atf1). AlkB, alkane monooxygenase; AlkG, rubredoxin; AlkT, rubredoxin reductase; AlkL, outer membrane protein. (b) The impact of co-expressing Crc with the diol synthesis pathway on the product formation in *E. coli*. Conversion tests were carried out with resting-cell conditions employing two *E. coli* strain backgrounds - NEBT7 and Top10. Error bars display standard deviation of biological triplicates. For each strain, conditions that do not share a letter are significantly different (Tukey test, adjusted p-value < 0.05). Total product levels were significantly different between conditions with and without Crc. (c) The expression levels of AlkS, AlkB, and AlkG in absence or presence of Crc. GFP was fused to the N-terminal of AlkS, AlkB, and AlkG to monitor their expression. AlkS is the activator of alkane degradation pathway. Error bars display standard deviation over three biological triplicates. Conditions that do not share a letter are significantly different (Tukey test, adjusted p-value < 0.05).

hexyl acetate suggests that, in the presence of Crc, the conversion from hexyl acetate to 6-hydroxyl hexyl acetate, mediated by AlkBGT, becomes a strong bottleneck in the pathway. To monitor their expression levels, AlkS, AlkB, and AlkG were fused separately to GFP. The expression of AlkB and AlkG was reduced when Crc was expressed in *E. coli* NEBT7 (Fig. 6c). This is consistent with observations that the activity of AlkBGT was strongly repressed. However, no significant difference was observed for the expression level of AlkS under the tested conditions. This may be related to its characteristic that, as an unstable protein, AlkS is present in a limited amount [30,47]. In contrast to the higher levels of hexyl-acetate, 1-hexanol and 6-hydroxyhexyl acetate were either non-detected or in lower concentrations, which indicates they were quickly converted by Atf1. This suggests that the impact of Crc on Atf1 activity was less. This is in line with its activity only being impacted by the Crc-Hfq mechanism via AlkS.

Another important aspect of AlkBGT is that it can also perform the overoxidation of 1-hexanol to hexanoic acid [31]. A high concentration of the latter would have conflicted with the inferred conclusion that Crc is inhibiting total product formation through repression of AlkBGT and Atf1 protein levels. To disregard this possibility, hexanoic acid concentrations were measured and found to be negligible (data not shown).

These results illustrate how a heterologous CCR mechanism of *P. putida*, particularly the presence of Crc, significantly reduced diester production in the host *E. coli*. The example of diester production demonstrates the feasibility of using Crc-Hfq as a tool for post-transcriptional multiplex regulation. Although off-target effects and Hfq shortage both need to be scrupulously dealt with, we provide evidence that Hfq shortage is likely of main importance. In principle, this can be countered by fine-tuning the expression of the Hfq protein together with Crc allowing for the native pool and functions of Hfq to be unaffected. Future work is needed to find a way to further mitigate these side effects. This method potentially provides advantages over other emerging methods such as transcription activator-like effector (TALE) and CRISPR interference (CRISPRi) in bacteria. The Crc-Hfq mechanism regulates gene expression post-transcriptionally. This can result in a much more immediate cellular response via direct regulation of protein concentration compared to methods based on transcriptional regulation. In addition, Hfq is present in many bacterial species [22], simplifying tool design and construction.

Conclusion

In this work, it is demonstrated for the first time that transplanting the pseudomonal catabolite repression Crc mechanism to a non-native host, *E. coli*, can serve as a tool for multiplex translation repression. The production of diol and its precursors was significantly reduced in presence of Crc. The expression of the Crc protein affected cell growth in both minimal and rich media via off-target effects and, especially, Hfq-sequestration. This can be mitigated by fine-tuning the expression level of Hfq and Crc. The introduction of the small mRNA CrcZ caused an even more severe reduction of the growth rate, indicating that a reduced Hfq pool plays a major role in the decrease of growth rate. This study sheds light on the feasibility of employing a heterologous regulation system to regulate gene expression.

CRediT authorship contribution statement

Conceptualization: **Chunzhe Lu**, and **Tiago P. Ramalho**; Investigation: **Chunzhe Lu**, and **Tiago P. Ramalho**; Data Analysis: **Tiago P. Ramalho**; Writing (original draft, reviewing and editing): **Chunzhe Lu**, **Tiago P. Ramalho**, **Markus M.M. Bisschops**, **Rene H. Wijffels**, **Vitor A.P. Martins dos Santos**, and **Ruud A. Weusthuis**; Supervision: **Ruud A. Weusthuis**.

Declaration of Competing Interest

The authors declare that they have no known competing financial interests or personal relationships that could have appeared to influence the work reported in this paper.

Acknowledgements

This work was supported by a Chinese Scholarship Council stipend (to C. Lu).

Appendix A. Supporting information

Supplementary data associated with this article can be found in the online version at doi:10.1016/j.nbt.2023.06.004.

References

[1] Vinuselvi P, Kim MK, Lee SK, Ghim CM. Rewiring carbon catabolite repression for microbial cell factory. BMB Rep 2012;45:59–70. https://doi.org/10.5483/BMBRep.2012.45.2.59.
[2] de Assis LJ, Silva LP, Bayram O, Dowling P, Kniemeyer O, Krüger T, et al. Carbon catabolite repression in filamentous fungi is regulated by phosphorylation of the transcription factor crea. MBio 2021;12:1–21. https://doi.org/10.1128/mBio.03146-20.
[3] Simpson-Lavy K, Kupiec M. Carbon catabolite repression in yeast is not limited to glucose. Sci Rep 2019;9:1–10. https://doi.org/10.1038/s41598-019-43032-w.
[4] Molina L, Rosa RLa, Nogales J, Rojo F. *Pseudomonas putida* KT2440 metabolism undergoes sequential modifications during exponential growth in a complete medium as compounds are gradually consumed. Environ Microbiol 2019;21:2375–90. https://doi.org/10.1111/1462-2920.14622.
[5] Görke B, Stülke J. Carbon catabolite repression in bacteria: many ways to make the most out of nutrients. Nat Rev Microbiol 2008;6:613–24. https://doi.org/10.1038/nrmicro1932.
[6] Stülke J, Hillen W. Carbon catabolite repression in bacteria. Curr Opin Microbiol 1999;2:195–201. https://doi.org/10.1016/S1369-5274(99)80034-4.
[7] Deutscher J. The mechanisms of carbon catabolite repression in bacteria. Curr Opin Microbiol 2008;11:87–93. https://doi.org/10.1016/j.mib.2008.02.007.
[8] Kremling A, Geiselmann J, Ropers D, de Jong H. Understanding carbon catabolite repression in *Escherichia coli* using quantitative models. Trends Microbiol 2015;23:99–109. https://doi.org/10.1016/j.tim.2014.11.002.
[9] Gerosa L, Haverkorn Van Rijsewijk BRB, Christodoulou D, Kochanowski K, Schmidt TSB, Noor E, et al. Pseudo-transition analysis identifies the key regulators of dynamic metabolic adaptations from steady-state data. Cell Syst 2015;1:270–82. https://doi.org/10.1016/j.cels.2015.09.008.
[10] Rojo F. Carbon catabolite repression in *Pseudomonas*: optimizing metabolic versatility and interactions with the environment. FEMS Microbiol Rev 2010;34:658–84. https://doi.org/10.1111/j.1574-6976.2010.00218.x.
[11] Kamilova F, Kravchenko LV, Shaposhnikov AI, Azarova T, Makarova N, Lugtenberg B. Organic acids, sugars, and L-tryptophane in exudates of vegetables growing on stonewool and their effects on activities of rhizosphere bacteria. Mol Plant-Microbe Inter 2006;19:250–6. https://doi.org/10.1094/MPMI-19-0250.
[12] Johnson CW, Abraham PE, Linger JG, Khanna P, Hettich RL, Beckham GT. Eliminating a global regulator of carbon catabolite repression enhances the conversion of aromatic lignin monomers to muconate in *Pseudomonas putida* KT2440. Metab Eng Commun 2017;5:19–25. https://doi.org/10.1016/j.meteno.2017.05.002.
[13] Moreno R., Marzi S., Romby P., Rojo F. The Crc global regulator binds to an unpaired A-rich motif at the *Pseudomonas putida* alkS mRNA coding sequence and inhibits translation initiation 2009;37:7678–90. https://doi.org/10.1093/nar/gkp825.
[14] Pei X.Y., Dendooven T., Sonnleitner E., Chen S., Luisi B.F. Architectural principles for Hfq/Crc-mediated regulation of gene expression 2019;8:1–20.
[15] Moreno R., Hernández-arranz S., Rosa R.La, Yuste L., Madhushani A., Shingler V., et al. The Crc and Hfq proteins of *Pseudomonas putida* cooperate in catabolite repression and formation of ribonucleic acid complexes with specific target motifs 2015;17:105–118. https://doi.org/10.1111/1462–2920.12499.
[16] Hernández-Arranz S, Moreno R, Rojo F. The translational repressor Crc controls the *Pseudomonas putida* benzoate and alkane catabolic pathways using a multi-tier regulation strategy. Environ Microbiol 2013;15:227–41. https://doi.org/10.1111/j.1462-2920.2012.02863.x.
[17] Rand JM, Pisithkul T, Clark RL, Thiede JM, Mehrer CR, Agnew DE, et al. A metabolic pathway for catabolizing levulinic acid in bacteria. Nat Microbiol 2017;2:1624–34. https://doi.org/10.1038/s41564-017-0028-z.
[18] Hsieh S., Wang J., Lai Y., Su C., Lee K. Production of 1-dodecanol, 1-tetradecanol, and 1,12- dodecanediol through whole-cell biotransformation in *Escherichia coli* 2018;84:1–12.
[19] Lu C, Batianis C, Akwafo EO, Wijffels RH, Martins dos Santos VAP, Weusthuis RA. When metabolic prowess is too much of a good thing: how carbon catabolite repression and metabolic versatility impede production of esterified α,ω-diols in

Pseudomonas putida KT2440. Biotechnol Biofuels 2021;14:1–15. https://doi.org/10.1186/s13068-021-02066-x.
[20] Moreno R, Fonseca P, Rojo F. Two small RNAs, CrcY and CrcZ, act in concert to sequester the Crc global regulator in *Pseudomonas putida*, modulating catabolite repression. Mol Microbiol 2012;83:24–40. https://doi.org/10.1111/j.1365-2958.2011.07912.x.
[21] Valentini M, García-Maurin SM, Pérez-Martínez I, Santero E, Canosa I, Lapouge K. Hierarchical management of carbon sources is regulated similarly by the CbrA/B systems in *Pseudomonas aeruginosa* and *Pseudomonas Putida*. Microbiol 2014;160:2243–52. https://doi.org/10.1099/mic.0.078873-0.
[22] Horstmann N., Orans J., Valentin-hansen P., Iii S.A.S., Brennan R.G. Structural mechanism of Staphylococcus aureus Hfq binding to an RNA A-tract 2012;40:11023–35. https://doi.org/10.1093/nar/gks809.
[23] Brosse A., Walburger A., Magalon A., Guillier M. Synthesis of the NarP response regulator of nitrate respiration in *Escherichia coli* is regulated at multiple levels by Hfq and small RNAs. BioRxiv 2021:2021.03.17.435884.
[24] Martínez LC, Vadyvaloo V. Mechanisms of post-transcriptional gene regulation in bacterial biofilms. Front Cell Infect Microbiol 2014:5. https://doi.org/10.3389/fcimb.2014.00038.
[25] Nakari-Setälä T, Paloheimo M, Kallio J, Vehmaanperä J, Penttilä M, Saloheimo M. Genetic modification of carbon catabolite repression in Trichoderma reesei for improved protein production. Appl Environ Microbiol 2009;75:4853–60. https://doi.org/10.1128/AEM.00282-09.
[26] Mello-de-Sousa TM, Gorsche R, Rassinger A, Poças-Fonseca MJ, Mach RL, Mach-Aigner AR. A truncated form of the carbon catabolite repressor 1 increases cellulase production in *Trichoderma reesei*. Biotechnol Biofuels 2014;7:1–12. https://doi.org/10.1186/s13068-014-0129-3.
[27] Fox KJ, Prather KL. Carbon catabolite repression relaxation in *Escherichia coli*: global and sugar-specific methods for glucose and secondary sugar co-utilization. Curr Opin Chem Eng 2020;30:9–16. https://doi.org/10.1016/j.coche.2020.05.005.
[28] Vo PNL, Lee H-M, Ren J, Na D. Optimized expression of Hfq protein increases *Escherichia coli* growth. J Biol Eng 2021;15:7. https://doi.org/10.1186/s13036-021-00260-x.
[29] Dinamarca MA, Aranda-Olmedo I, Puyet A, Rojo F. Expression of the *Pseudomonas putida* OCT plasmid alkane degradation pathway is modulated by two different global control signals: evidence from continuous cultures. J Bacteriol 2003;185:4772–8. https://doi.org/10.1128/JB.185.16.4772-4778.2003.
[30] Moreno R, Ruiz-Manzano A, Yuste L, Rojo F. The *Pseudomonas putida* Crc global regulator is an RNA binding protein that inhibits translation of the AlkS transcriptional regulator. Mol Microbiol 2007;64:665–75. https://doi.org/10.1111/j.1365-2958.2007.05685.x.
[31] van Nuland YM, de Vogel FA, Scott EL, Eggink G, Weusthuis RA. Biocatalytic, one-pot diterminal oxidation and esterification of n-alkanes for production of α,ω-diol and α,ω-dicarboxylic acid esters. Metab Eng 2017;44:134–42. https://doi.org/10.1016/j.ymben.2017.10.005.
[32] Lu C, Leitner N, Wijffels RH, Martins VAP, Weusthuis A. Microbial production of medium-chain-length α, ω-diols via two-stage process under mild conditions. Bioresour Technol 2022;352:127111. https://doi.org/10.1016/j.biortech.2022.127111.
[33] Green R, Rogers EJ. Chemical transformation of *E. coli*. methods Enzym 2013;529:329–36. https://doi.org/10.1016/B978-0-12-418687-3.00028-8.Chemical.
[34] Green R, Rogers EJ. Transformation of chemically competent *E. coli*. Methods Enzymol, vol. 529. Academic Press Inc,; 2013. p. 329–36. https://doi.org/10.1016/B978-0-12-418687-3.00028-8.
[35] Julsing MK, Schrewe M, Cornelissen S, Hermann I, Schmid A, Bühler B. Outer membrane protein alkL boosts biocatalytic oxyfunctionalization of hydrophobic substrates in *Escherichia coli*. Appl Environ Microbiol 2012;78:5724–33. https://doi.org/10.1128/AEM.00949-12.
[36] Bohnenkamp AC, Kruis AJ, Mars AE, Wijffels RH, Van Der Oost J, Kengen SWM, et al. Multilevel optimisation of anaerobic ethyl acetate production in engineered *Escherichia coli*. Biotechnol Biofuels 2020;13:1–14. https://doi.org/10.1186/s13068-020-01703-1.
[37] van Nuland YM, de Vogel FA, Eggink G, Weusthuis RA. Expansion of the ω-oxidation system AlkBGTL of *Pseudomonas putida* GPo1 with AlkJ and AlkH results in exclusive mono-esterified dicarboxylic acid production in *E. coli*. Micro Biotechnol 2017;10:594–603. https://doi.org/10.1111/1751-7915.12607.
[38] Bohnenkamp AC, Wijffels RH, Kengen SWM, Weusthuis RA. Co-production of hydrogen and ethyl acetate in *Escherichia coli*. Biotechnol Biofuels 2021;14:1–12. https://doi.org/10.1186/s13068-021-02036-3.
[39] Verduyn C, Postma E, Scheffers WA, Van Dijken JP. Effect of benzoic acid on metabolic fluxes in yeasts: a continuous-culture study on the regulation of respiration and alcoholic fermentation. Yeast 1992;8:501–17. https://doi.org/10.1002/yea.320080703.
[40] Lu C, Akwafo EO, Wijffels RH, Martins dos Santos VAP, Weusthuis RA. Metabolic engineering of *Pseudomonas putida* KT2440 for medium-chain-length fatty alcohol and ester production from fatty acids. Metab Eng 2023;75:110–8. https://doi.org/10.1016/j.ymben.2022.11.006.
[41] Kim SK, Seong W, Han GH, Lee DH, Lee SG. CRISPR interference-guided multiplex repression of endogenous competing pathway genes for redirecting metabolic flux in Escherichia coli. Micro Cell Fact 2017;16:188. https://doi.org/10.1186/s12934-017-0802-x.
[42] Bharwad K, Rajkumar S. Rewiring the functional complexity between Crc, Hfq and sRNAs to regulate carbon catabolite repression in *Pseudomonas*. World J Microbiol Biotechnol 2019;35:1–12. https://doi.org/10.1007/s11274-019-2717-7.
[43] Molina L, La Rosa R, Nogales J, Rojo F. Influence of the Crc global regulator on substrate uptake rates and the distribution of metabolic fluxes in *Pseudomonas putida* KT2440 growing in a complete medium. Environ Microbiol 2019;21:4446–59. https://doi.org/10.1111/1462-2920.14812.
[44] Yang S, Pelletier DA, Lu TYS, Brown SD. The *Zymomonas mobilis* regulator hfq contributes to tolerance against multiple lignocellulosic pretreatment inhibitors. BMC Microbiol 2010;10:135. https://doi.org/10.1186/1471-2180-10-135.
[45] Jungfleisch J, Chowdhury A, Alves-Rodrigues I, Tharun S, Díez J. The Lsm1-7-Pat1 complex promotes viral RNA translation and replication by differential mechanisms. RNA 2015;21:1469–79. https://doi.org/10.1261/rna.052209.115.
[46] Moon K, Gottesman S. Competition among Hfq-binding small RNAs in *Escherichia coli*. Mol Microbiol 2011;82:1545–62. https://doi.org/10.1111/j.1365-2958.2011.07907.x.
[47] Yuste L, Rojo F. Role of the crc gene in catabolic repression of the *Pseudomonas putida* GPo1 alkane degradation pathway. J Bacteriol 2001;183:6197–206. https://doi.org/10.1128/JB.183.21.6197-6206.2001.